The final publication is available at

http://ascelibrary.org/doi/10.1061/(ASCE)BE.1943-5592.0000896

Additional Information

1 **Evaluation of transverse impact factors in twin-box girder bridges for high-speed**

2 **railways**

3 Emma Moliner[a]*, José Lavado[b], Pedro Museros[c,d]

4

5 **Abstract**

6 This paper deals with the dynamic behavior of twin-box girder bridges under high-speed
7 railway traffic. Based on several representative examples derived from recently built high-
8 speed bridges, this contribution examines the effects of transverse bending in the upper slab
9 of these structures and evaluates the bending moments in resonance conditions. The analysis
10 is carried out according to one of the reference norms for the assessment of dynamic effects in
11 high-speed bridges (Eurocode). The results demonstrate that the predicted dynamic response
12 for shorter span bridges could be unexpectedly higher than the static effects caused by the
13 design loads, due to transverse resonances induced by the absence of transverse diaphragms
14 between the box girders and the movement of the sliding supports. Moreover, these strong
15 impact coefficients may occur even when the maximum level of vertical vibrations in the
16 deck is not alarming.

17

18 *[a]*Assistant Professor PhD, Department of Mechanical Engineering and Construction, Universitat Jaume I, Avda Sos Baynat*
19 *s/n, 12071 Castellón, Spain (Corresponding author). Email:* molinere@uji.es

20 *[b]Associate Professor, Department of Structural Mechanics and Hydraulic Engineering, Universidad de Granada, Campus*
21 *Universitario de Fuentenueva, 18071, Granada, Spain.*

22 *[c]Associate Professor, Department of Continuum Mechanics and Theory of Structures, Universitat Politècnica de València,*
23 *Camino de Vera s/n, 46022 Valencia, Spain.*

24 *[d]Fundación Caminos de Hierro para la Investigación y la Ingeniería Ferroviaria, C/ Serrano 160, 28002 Madrid, Spain.*

25

26

27

28 **Introduction**

29   In modern high-speed railway lines *twin-box girder bridges* have become one of the

30 most popular solutions for spans between approximately 20 m and 45 m (Figure 1). This

31 success is attributable to their short construction time, which is largely due to the

32 prefabrication of the two main girders.

33   Significant dynamic effects may arise when transversely movable supports are

34 deployed in absence of diaphragms between the box girders. This configuration, which can be

35 found in high-speed lines such as the one connecting Spain and France or Madrid and

36 Barcelona (Burón and Peláez, 2002), induces potential resonance responses of the structure

37 that could seriously affect the upper concrete slab (excessive cracking, fatigue) if the dynamic

38 effects are not considered properly.

39   Some earlier studies on the subject do deal with transverse bending (Hamed and

40 Frostig 2005, Huang and Wang 1993, 1995, Rattigan et al. 2005), but very little has been said

41 about twin-box girder bridges. Cheung and Megnounit (1991) conducted a study specifically

42 devoted to twin-box girder bridges. However it fails to consider the transverse distribution of

43 bending moments.

44   This work endeavors to launch a comprehensive study where several twin-box girder

45 bridges of increasing span length are analyzed. The numerical models used in this study

46 intentionally follow the prescriptions of Eurocode 1 (EC1) (CEN, EN 1991-2 2002), in an

47 attempt to show the predicted performance at the design stage. The influence of the

48 configuration of the supports on the dynamic response, particularly in the absence of

49 transverse diaphragms between the main girders, is one of the key issues with which this

50 paper is concerned.

Twin-box girder bridges: case studies

This study presents analysis results for four simply-supported decks of spans (20, 25, 30 and 35 m). Their main properties, shown in Figure 2 and Table 1, are derived from existing structures so as to constitute realistic examples leading to meaningful results and conclusions. The bridge deck consists of two prestressed, precast concrete U-shaped girders and a reinforced concrete, cast in-situ upper slab. Each U-girder usually has rigid diaphragms at both ends, where the hollow section is stiffened by a solid infill.

As regards the longitudinal constraints, both pots at one end are fixed and those at the opposite end are free. In a generic manner, the end of the deck where the longitudinal constraints are placed is referred to as *fixed abutment*.

Numerical model

General aspects and assumptions

Two different linear elastic analyses were performed: static and transient dynamic analysis solved by mode superposition under the action of railway traffic. With this purpose a suitable finite element model (FEM) was devised. The meshing process, the static analyses and the extraction of frequencies and mode shapes were performed using the commercial code ANSYS, while the intensive computations associated with the passing of trains across the bridges at different speeds were implemented with a suitable FORTRAN routine. This routine carries out the time-integration by the Newmark-β linear acceleration algorithm, using a time step equal to 1/25 times the smallest period among the modes considered.

A point load model is adopted for the railway excitation, following the European standards. Therefore, train-bridge interaction is neglected in the analysis, which is also supported by previous works (Doménech et al. 2014). The numerical model also disregards track irregularities, since the regulations merely treat them by means of a multiplying factor.

75   The effects of soil-structure interaction are also neglected; this is usual in bridges supported

76   on short piles lying on a stiff foundation (Antolín et al. 2013; Liu et al. 2014).

77

78   ***Deck geometry***

79   Figure 3 shows the mesh in the area near the abutments. The structure is discretized using

80   four-node shell elements with six degrees of freedom (dofs) per node and out-of-plane shear

81   deformation capabilities. For the rigid diaphragms at both ends of the girders (shaded

82   elements in Figure 3), eight-node hexahedral solid elements with three dofs per node were

83   used.

84   All the elements have a length of 0.25 m in direction X. The size along direction Y

85   (slabs) and direction Z (webs) does not remain constant for all the span lengths, but is rather

86   similar. The average length in direction Y is 0.22 m for the upper slab and 0.14 m for the

87   lower slab. Along the webs the average size is 0.18 m.

88   Permanent loads, e.g., ballast, track, walkways, etc., are distributed as additional

89   masses of the elements of the upper slab. As regards the boundary conditions, the model

90   considers pot bearings as ideal supports, a common assumption that previous research works

91   also adopted (Majka and Hartnett 2009; Antolín et al. 2013). In the fixed abutment the bottom

92   center node of the solid meshes at the diaphragm positions in each of the girders is

93   constrained in the longitudinal and vertical directions (X and Z), whereas only one of them is

94   fixed in transverse direction Y. At the opposite abutment the boundary conditions are

95   identical except for the constraints in X, which are not present. Additionally, kinematic

96   constraints are used in order to tie this restrained central node to a number of adjacent

97   rows/columns of nodes, covering an area similar to the real pot dimensions.

98   *Static and dynamic loads*

99   From a practical point of view it is customary to refer the maximum dynamic effects to some

100   particular static load scenario by means of the so-called *impact coefficients*, i.e. the ratio

101   between maximum dynamic and static values of the internal forces. As a common practice in

102   Europe, the reference static forces to be applied are the UIC-71 train defined in EC1, which

103   represents the static effect of vertical loading due to normal rail traffic. In this study the

104   variables of real interest are the dynamic internal forces; therefore the UIC-71 loads are

105   located in a convenient, straightforward position, acting symmetrically with respect to the

106   mid-span section.

107   The most unfavorable dynamic load usually occurs when the trains circulate at speeds

108   such that a given vibration mode experiences resonance. According to EC1 only one loaded

109   track is considered during the dynamic analyses, and the dynamic loads to be applied are the

110   10 trains prescribed in the High Speed Load Model A (HSLM-A model). They constitute an

111   envelope of the dynamic effects of the existing conventional high-speed trains.

112   **Description of the analyses and post-processing points**

113   The response of the four subject bridges is computed first in terms of transverse bending

114   moments under the static action of the UIC-71 loads placed at mid-span. These response

115   variables are then evaluated under the circulation of HSLM-A trains along each of the tracks

116   on the bridge (track I and track II, according to Figure 2) in two different ranges of velocities

117   of interest, which are [72, 420] km/h and [72, 540] km/h in steps of 3.6 km/h. The impact

118   coefficients are evaluated separately in each range of circulation speeds.

119   The static and dynamic results are computed at five sections {A, B, C, D, E}

120   corresponding to x/L = {0.25, 0.375, 0.5, 0.625, 0.75}, where L is the span length. In each

121   section several points for obtaining bending moments and also vertical accelerations are

122   considered. Figure 2 shows the locations of the points: transverse bending moments are

123 computed at points from 1 to 9, and accelerations are obtained at points 11, 10, 5 and 12.

124 Notice that when the loaded track is I, point 10 is located between points 2 and 3; conversely,

125 if the loaded track is II, point 10 is placed between 7 and 8.

126 **Results**

127 *Natural frequencies and mode shapes*

128 All the cases of study have a similar pattern in their mode shapes: the first three

129 eigenforms are global ones and they essentially govern the dynamic response; the modes

130 above the third one may be local or global, and their main effect on the internal forces is a

131 pseudo-static contribution. Table 2 gathers the natural frequencies of the first four eigenforms.

132 Figure 4 shows the first four modes and their frequencies for the 25 m bridge. The first

133 mode is a transverse bending of the upper slab. In this eigenform the girders rotate as rigid

134 bodies and have little torsion, with also a limited longitudinal bending. In longitudinal

135 bending the U-girders do not behave as a single beam, but their main bending vibrations

136 correspond to modes 2 and 3 with similar frequencies and shapes: in both modes there is a

137 predominant longitudinal bending of one of the U-girders, complemented by a kind of rigid-

138 body rotation and a limited bending of the other. The bridges of span 20 m, 30 m and 35 m

139 feature similar mode shapes.

140 *Envelopes of internal forces versus speed*

141 Figure 5 shows the maximum absolute values of transverse bending moment (M_x) due

142 to the circulation of the HSLM-A trains at the most unfavorable post-process points. The

143 values are plotted against the circulating speed for all bridges and for an increasing number of

144 mode contributions (up to 200 modes, showing a satisfactory convergence). These results

145 correspond to the circulation of the trains along track I, and a uniform damping ratio of 1% is

146 assigned to all mode contributions following the prescriptions of EC1. For the sake of

147   comparison, Figure 5 also shows the maximum absolute static value among all the post-

148   process points under the action of the UIC-71 train. Particularly for the shortest structures, the

149   maximum dynamic values largely exceed the static ones created by the UIC-71 design loads.

150   As can be seen in Figure 5, the maximum resonance peaks of the transverse bending

151   moments are mainly governed by the contribution of the first eigenform at speeds below

152   300–350 km/h, which is a frequent velocity limit in many high-speed railway lines. The

153   contribution of the longitudinal bending modes is also noticeable at speeds higher than 350

154   km/h, especially for the shortest spans (L= 20 m, 25 m); but as the span length increases, the

155   first mode prevails.

156   When the trains circulate along the opposite track (track II) the predominant mode

157   contributions for each span length do not differ significantly from the results shown in Figure

158   5. However, the influence of the loaded track on the dynamic response amplitude is in general

159   quite noticeable. This is shown in Figure 6(a), where the transverse bending moment at the

160   critical post-process points for the bridge of 25 m span is plotted, considering the contribution

161   of the first 200 modes and the circulation of the trains alternatively along track I and track II,

162   in opposite directions. These results highlight that the dynamic behavior of twin-box girder

163   bridges under moving loads is clearly three-dimensional.

164   ***Impact coefficients***

165   On a standard basis, the impact coefficients for transverse bending moments are used

166   for the design of the transverse reinforcement in the upper slab. In the initial design stages of

167   twin-box girder bridges, the coefficients presented in this section may thus provide a helpful

168   first estimate of what may be expected from transverse resonance phenomena.

169   The impact coefficient is evaluated as the quotient between the maximum dynamic

170   value in the upper slab and the maximum static one, both of them having the same sign. The

171 maximum static values used for the evaluation of the impact factors are obtained after placing

172 UIC-71 loads symmetrically along track II. The maximum dynamic transverse bending

173 moments in the upper slab are positive, and are caused by the circulation of the trains along

174 track I. They have been collected in Figure 7.

175   Table 3 gathers the impact coefficients for the bending moment considering maximum

176 train speeds of 420 km/h and 540 km/h. It is seen that they are more affected by the increase

177 in speed for the shortest span, while they remain almost constant when the velocity rises to

178 540 km/h for the longest spans. Values higher than 2.0 are obtained in several cases. If not

179 taken properly into account, this effect may have an influence on the transverse cracking of

180 the concrete slab, which in turn may result in reductions in both the stiffness and the first

181 natural frequency, thus leaving the bridge even more exposed to resonance phenomena (at

182 lower speeds).

183 ***Vertical accelerations***

184   The maximum level of vertical vibrations usually constitutes a critical Serviceability

185 Limit State (SLS) for other types of simply-supported high-speed bridges (ERRI D214/RP9

186 2001; Frýba 2001; EN 1991-2 2002; Museros and Alarcón 2005). The vertical accelerations

187 under the circulation of HSLM-A trains have been computed considering a maximum number

188 of mode contributions up to 30 Hz, which is a limit usually prescribed by structural codes

189 (ERRI D214/RP9 2001). The maximum peak values of the vertical acceleration of the bridge

190 deck calculated along each track shall not exceed 3.5 m/s^2 for ballasted tracks, according to

191 Eurocode (CEN, EN 1990-A2, 2005).

192   The analyses have shown that the 35 m bridge satisfies the 3.5 m/s^2 criterion in the

193 whole range of speeds. The 30 m bridge presents a good behavior up to 400 km/h

194 approximately. The 20 and 25 m bridges also behave well up to 350 km/h (approx.), where

195 resonances of the second and third modes start to increase the response significantly.

196 Consequently, the potential use of twin-box girder bridges for *very high-speed* lines (V>350

197 km/h) should be examined with particular care.

198   Finally, Figure 6(b) shows the influence of the loaded track on the envelopes of

199 maximum acceleration versus speed, for the 25 m bridge. The most unfavorable circulating

200 track is not the same over the whole range of speeds, a fact that was also observed for

201 transverse bending moments, and underlines the importance of using three-dimensional

202 models in the dynamic analysis of this type of bridge.

203 **Conclusions**

204 In this work the dynamic response of several representative twin-box girder bridges under

205 high-speed railway traffic has been analyzed. The aim of this study was to investigate the

206 unusual performance predicted at the design stage when the transversally sliding bearings

207 beneath one of the U-girders are modelled as ideal rollers and without transverse diaphragms

208 between the box girders. The main conclusions are the following:

209 • The impact coefficients for transverse bending moments are higher than 2.0 and tend

210   to decrease with the span length. Such extreme values highlight the need for future

211   research work to support or contradict whether they are excessively conservative due

212   to other effects that should be considered in the calculations, such as a performance of

213   the pot bearings far from the ideal behavior implemented in most numerical models.

214 • At speeds below 350 km/h the transverse bending moments are mainly governed by

215   resonances of the first eigenform. The introduction of diaphragms or cross-bracings

216   between the girders could significantly reduce those transverse bending moments in

217   spite of a certain amount of complexity being added to the construction process. This

218   stiffening measure would be in line with the California codal recommendation of the

219   first torsional frequency being at least 1.2 times greater than the first vertical bending

220   frequency. Such interpretation of this code would be reasonable from an engineering

221   point of view, given that the first eigenform is not a torsional mode but a transverse

222   bending one that is not contemplated in (California High-Speed rail Authority 2014).

223   • The potential use of twin-box girder bridges for very high-speed lines (V>350 km/h

224   approx.) should be examined with particular care due to excessively high vertical

225   accelerations appearing in the ballast. Structures that are stiffer and more massive than

226   the ones analyzed in this paper could be required to satisfy the acceleration SLS

227   ($3.5 \ \mathrm{m/s^2}$) at such very fast speeds.

228   • The dynamic behavior of twin-box girder bridges under moving loads is clearly three-

229   dimensional: the contribution of the first transverse bending mode to the

230   corresponding bending moments and the influence of the loaded track are significant.

236 **References**

237 Antolín, P, Zhang, N, Goicolea, J.M., Xia, H, Astiz, M.A. and Oliva J. (2013). "Consideration

238 of nonlinear wheel–rail contact forces for dynamic vehicle–bridge interaction in high-speed

239 railways". J Sound Vib, 332, 1231-1251.

240 Burón M., Peláez. (2002). "Puentes para el ferrocarril de alta velocidad con tablero

241 prefabricado". II Congreso de ACHE de Puentes y Estructuras, Madrid.

242 CEN (2002). EN 1991-2. *Eurocode 1: Actions on Structures - Part 2: Traffic loads on*

243 *bridges*. Brussels: European Committee for Standardization.

244 CEN (2005). EN 1990-A2. *Eurocode: Basis of structural design*. Annex A2, application for
245 bridges. Final version. Brussels: European Committee for Standardization.

246 California High-Speed rail Authority (2014). Request for proposals for Design-Build Services
247 for Construction Package 2-3. Book III, Part A, Design criteria manual. Rapport nº: HSR 13-
248 57.

249 Cheung, M.S., and Megnounit, A. (1991). "Parametric study of design variations on the
250 vibration modes of box girder bridges". Canadian Journal of Civil Engineering, 18, 789-798.

251 Doménech, A., Museros, P., Martínez-Rodrigo, M.D. (2014). "Influence of the vehicle model
252 on the prediction of the maximum bending response of simply-supported bridges under high-
253 speed railway traffic". Engineering Structures, 72, 123-139.

254 ERRI D214/RP9 (2001). Railway bridges for speeds>200 km/h. (Final Report) Utrecht:
255 European Rail Research Institute (ERRI).

256 Frýba L. (2001) "A rough assessment of railway bridges for high speed trains". Eng Struct,
257 23, 548–556.

258 Hamed, E., and Frostig, Y. (2005). "Free vibrations of multi-girder and multi-cell box bridges
259 with transverse deformations effects". J Sound Vib, 279, 699-722.

260 Huang, D., Wang, T.L., and Shahawy, M. (1993). "Impact studies of multigirder concrete
261 bridges". Journal of Structural Engineering, ASCE, 119, 2387-2402.

262 Huang, D., Wang, T.L., and Shahawy, M. (1995). "Vibration of thin-walled box-girder
263 bridges excited by vehicles". Journal of Structural Engineering, ASCE, 121, 1330-1337.

264 Liu K, Lombaert G, and De Roeck G. (2014). "Dynamic analysis of multispan viaducts with
265 weak coupling between adjacent spans". Journal of Bridge Engineering, 19, 83-90.

266 Majka, M., and Hartnett, M. (2009). "Dynamic response of bridges to moving trains: A study
267 on effects of random track irregularities and bridge skewness". Computers & Structures, 87,
268 1233-1252.

269 Rattigan, P.H., González, A., O'Brien, E.J., and Brady S.P. (2005). "Transverse variation of
270 dynamic effects on beam-and-slab medium span bridges". In Proceedings of the sixth
271 European conference on structural dynamics, 1643-1648.

272

273

274

275

276

277 **Figure captions**

278

279 **Fig. 1.** Twin-box girder bridge on Madrid-Barcelona high-speed railway line. Characteristic

280 span length L=30 m

281 **Fig. 2.** Representative cross-section of a twin-box girder bridge and post-process points

282 **Fig. 3.** FE mesh at the fixed abutment

283 **Fig. 4.** First four vibration modes for the 25 m bridge

284 **Fig. 5.** Envelopes of maximum absolute transverse bending moments due to live loads. Trains

285 circulating along track I. Legend in (d) applies to all subplots.

286 **Fig. 6.** Envelopes of maximum dynamic results for the 25 m bridge. (a) Transverse bending

287 moments; (b) vertical accelerations.

288 **Fig. 7.** Envelopes of maximum positive transverse bending moments under the circulation of

289 HSLM-A trains along tracks I and II. (a_i) V_{max}=350 x1.2=420 km/h; (b_i) V_{max}=450 x 1.2=540

290 km/h.

291

292

293

294

295

L (m)		20	25	30	35
Upper slab	ρ (kg/m³)		2500		
	f_{ck} (MPa)		35		
U-girders	h_u (m)	1.44	1.89	2.35	2.8
	ρ (kg/m³)		2500		
	f_{ck} (MPa)		45		
Dead loads	*Ballast+tracks* (kg/m)		11000		
	Walls (kg/m)		480		
	Walkways (kg/m)		2450		
	Handrails (kg/m)		900		

296   **Table 1.** Main properties of the bridges

297

L (m)	1ˢᵗ mode	2ⁿᵈ mode	3ʳᵈ mode	4ᵗʰ mode
20	4.141	5.750	6.230	9.288
25	3.671	4.991	5.741	8.803
30	3.232	4.335	5.512	8.191
35	2.862	3.822	5.329	7.428

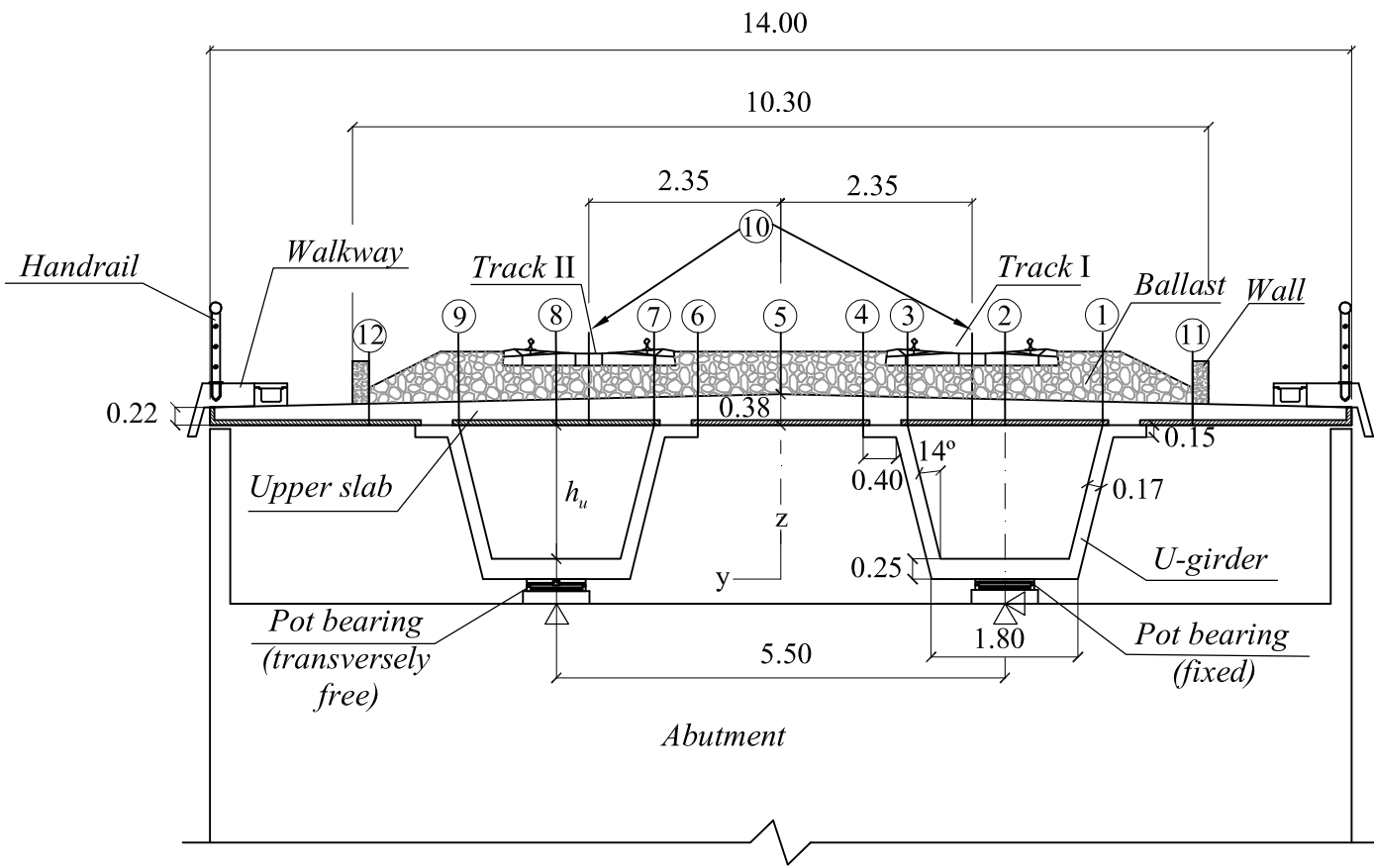298   **Table 2.** First four natural frequencies (Hz) of the bridges

299

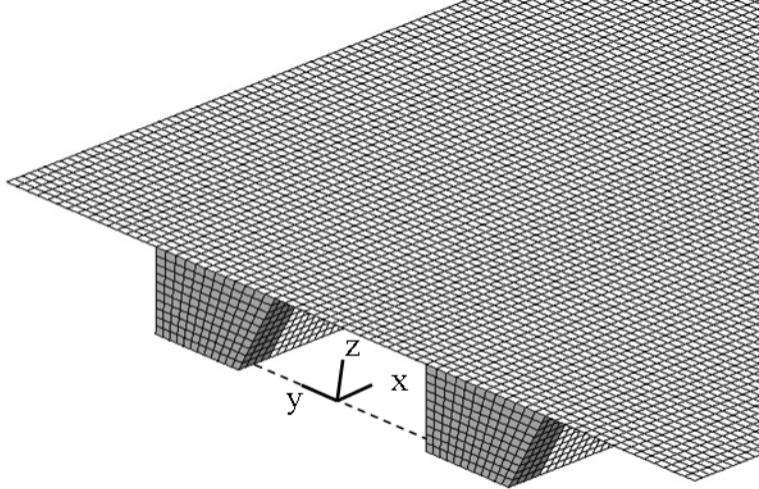| V_{max}	L=20 m	L=25 m	L=30 m	L=35 m
420 km/h	2.54	2.11	1.41	0.98
540 km/h	3.39	2.11	1.41	0.98

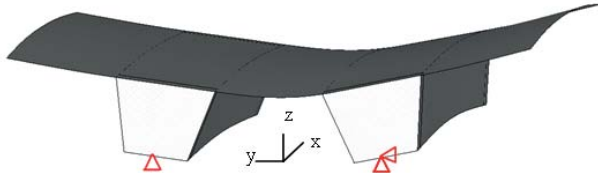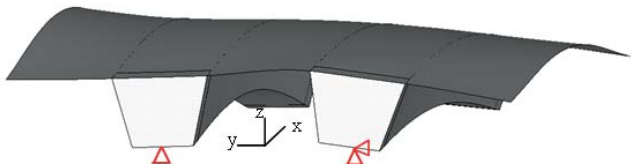300   **Table 3.** Impact coefficients for transverse bending moment
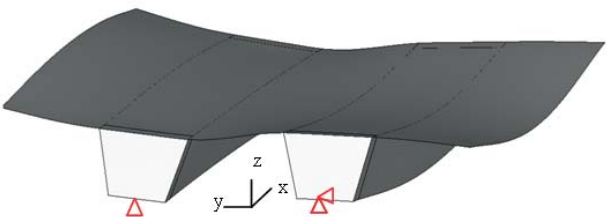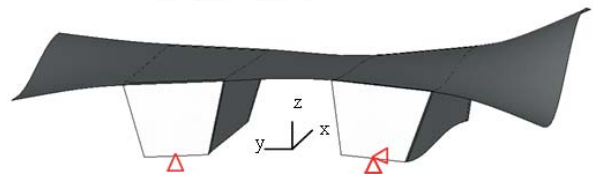
301

Mode 1: f=3.67 Hz

Mode 2: f=4.99 Hz

Mode 3: f=5.74 Hz

Mode 4: f=8.80 Hz

(a)

Trains circulating along track I
Trains circulating along track II

Maximum M_x (kN·m/m)

UIC-71

A4

A4

(b)

Vertical acceleration (m/s²)

3.5 m/s²

C12

C11

V (km/h)

Maximum M_x (kN·m/m)

A ■ B ■ C ■ D □ E

(a_1) (a_2) (a_3) (a_4)

(b_1) (b_2) (b_3) (b_4)

L=20 m L=25 m L=30 m L=35 m